Acta Crystallographica Section D
Biological Crystallography
ISSN 0907-4449

Structure of ribosomal protein L1 from *Methanococcus thermolithotrophicus*. Functionally important structural invariants on the L1 surface

Natalia Nevskaya,[a] Svetlana Tishchenko,[a] Mikhail Paveliev,[a] Yulia Smolinskaya,[a] Roman Fedorov,[a] Wolfgang Piendl,[b] Yoshikazu Nakamura,[c] Tomohiko Toyoda,[c] Maria Garber[a] and Stanislav Nikonov[a]*

[a]Institute of Protein Research, Russian Academy of Sciences, 142290 Pushchino, Moscow Region, Russia, [b]Institute of Medical Chemistry and Biochemistry, University of Innsbruck, Austria, and [c]Department of Tumor Biology, The Institute of Medical Science, University of Tokyo, Japan

Correspondence e-mail: nikonov@vega.protres.ru

Received 10 December 2001
Accepted 8 April 2002

PDB Reference: ribosomal protein MthL1, 1dwu, r1dwusf.

The crystal structure of ribosomal protein L1 from the archaeon *Methanococcus thermolithotrophicus* has been determined at 2.7 Å resolution. The crystals belong to space group $P2_12_12_1$, with unit-cell parameters a = 67.0, b = 70.1, c = 106.3 Å and two molecules per asymmetric unit. The structure was solved by the molecular-replacement method with *AMoRe* and refined with *CNS* to an R value of 18.9% and an $R_{\rm free}$ of 25.4% in the resolution range 30–2.7 Å. Comparison of this structure with those obtained previously for two L1 proteins from other sources (the bacterium *Thermus thermophilus* and the archaeon *M. jannaschii*) as well as detailed analysis of intermolecular contacts in the corresponding L1 crystals reveal structural invariants on the molecular surface which are probably important for binding the 23S ribosomal RNA and protein function within the ribosome.

1. Introduction

Ribosomal protein L1 is one of the largest ribosomal proteins. L1 from *Escherichia coli* associates independently and specifically with the 23S rRNA and protects a fragment of approximately 100 nucleotides against nuclease digestion (Zimmermann, 1980; Branlant *et al.*, 1981). The primary and secondary structures of the L1-binding region on the 23S and 28S rRNA are highly conserved in bacteria, archaea and eukarya (Zimmermann *et al.*, 1980; Gourse *et al.*, 1981). It has been shown that in bacteria and archaea this protein is also able to regulate gene expression by binding to its own mRNA, thereby acting as a translation repressor (Gourse *et al.*, 1986; Kraft *et al.*, 1999).

Crystal structures of two L1 proteins, those from the bacterium *Thermus thermophilus* (TthL1) and the archaeon *Methanococcus jannaschii* (MjaL1), have been already determined at 1.85 Å (Nikonov *et al.*, 1996) and 2.3 Å resolution (Nevskaya *et al.*, 2000), respectively. The structure of MjaL1 was subsequently refined to 1.85 Å resolution using data from crystals cooled to 100 K (PDB code 1i2a). A comparison of the TthL1 and MjaL1 structures (29.1% sequence identity) revealed some interesting features. Both domains of these proteins retain a close topology, whereas the overall shapes of the molecules differ dramatically owing to different relative orientations of the domains in both structures. As a result, MjaL1 has a more open conformation stabilized by a complex network of interdomain interactions. Attempts to fit the structure of TthL1 into the electron-density maps of the 50S ribosomal subunit of *Haloarcula marismortui* failed, whereas the structure of MjaL1 could be positioned in the 12 Å resolution map of the large ribosomal subunit; nevertheless, it was not seen in higher resolution maps (Ban *et al.*, 1999, 2000). The

5.5 Å resolution model of the *T. thermophilus* 50S ribosomal subunit (Yusupov *et al.*, 2001) contains the TthL1 structure. However, this model includes only the C^{α} atoms of protein L1 and the P atoms of 23S rRNA; the location of protein L1 cannot be treated as reliable as its C^{α}- and P-atom traces are partly overlapped (PDB code 1giy).

In this paper, we report the structure of the L1 protein from the archaeon *M. thermolithotrophicus* (MthL1). Comparison of this structure with the structures of TthL1 and MjaL1 reveals structural invariants on the surface of the L1 molecule. These regions are involved in the intermolecular interactions in the crystals and may be important for protein function.

2. Experimental

2.1. Crystallization and data collection

Ribosomal protein L1 from *M. thermolithotrophicus* overproduced in *E. coli* (Köhrer *et al.*, 1998) was purified by cation-exchange chromatography as reported for L1 from *M. jannaschii* (Tishchenko *et al.*, 1998). Fractions containing pure MthL1 were pooled, precipitated with ammonium sulfate and dialyzed against the buffer 66 m*M* $MgCl_2$, 70 m*M* NaCl, 70 m*M* CH_3COONa pH 5.5. Crystallization experiments were performed at 277 K using the hanging-drop vapour-diffusion method on siliconized glass cover slides in Linbro plates. Initial crystallization conditions were found using Crystal Screen I (Hampton Research). Crystals of MthL1 were obtained when 4 µl of the protein solution at a concentration of 25–30 mg ml^{-1} was mixed with 2 µl of precipitant buffer No. 22 of Crystal Screen I (30% PEG 4K, 0.1 *M* Tris–HCl pH 8.5, 0.2 *M* CH_3COONa) and equilibrated against 30% PEG 4K, 0.1 *M* CH_3COONa pH 5.5. The crystals appeared after 2–3 d and grew to maximum dimensions of 1 × 0.15 × 0.2 mm within one week.

Table 1
Data-collection statistics.

Values for the highest resolution shell are shown in parentheses.

Space group	$P2_12_12_1$
Unit-cell parameters (Å)	a = 67.0, b = 70.1, c = 106.3
Resolution range (Å)	30–2.7
Unique reflections	14280
Completeness (%)	94.6 (81.7)
Redundancy	4.31 (3.8)
R_{merge} (%)	7.0 (27.5)

The crystals belong to space group $P2_12_12_1$, with unit-cell parameters a = 67.0, b = 70.1, c = 106.3 Å, and diffract to 2.7 Å resolution. Diffraction data were collected at room temperature on a Rigaku R-AXIS IV imaging-plate detector system using Cu $K\alpha$ radiation from a Rigaku Ru-H3RHB rotating-anode generator (Tokyo, Japan) operating at 50 kV and 80 mA. All data were processed and merged with *DENZO* and *SCALEPACK* programs (Otwinowski & Minor, 1997). Data statistics are summarized in Table 1.

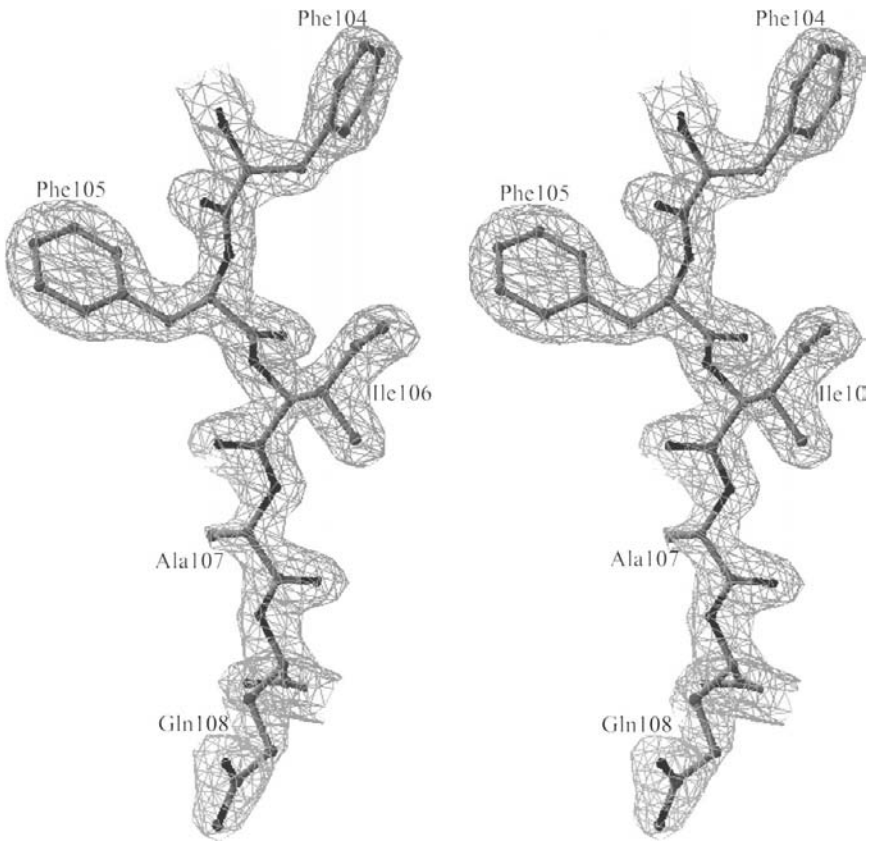

Figure 1
Stereoview showing the final $2F_o - F_c$ map at 2.7 Å resolution contoured at the 1σ level. Figures were produced with *MolScript* (Kraulis, 1991), *BobScript* (Esnouf, 1999), *WebLab ViewerPro* (WebLab ViewerLite 3.20, Molecular Simulations Inc.) and *POV-Ray* (Persistence of Vision Ray Tracer v3.02, POV-Team; http://www.povray.org).

2.2. Molecular replacement and refinement

The MthL1 and MjaL1 amino-acid sequences demonstrate 71.4% identity. This allowed the use of the molecular-replacement method to solve the phase problem. The structure of MthL1 was solved with the *AMoRe* package (Navaza, 1994) using the partly modified model of MjaL1 as a search model. From crystal density considerations (Matthews, 1968), two molecules were considered to be present in the asymmetric unit. Peaks in the cross-rotation function used for a two-body translation-function search with a subsequent rigid-body refinement gave a highly contrasted peak with a correlation coefficient of 60.6% and an R factor of 40.6%, while a second peak had corresponding values of 42.0 and 48.1%. The initial map enabled us to construct a

complete model of both molecules in the asymmetric unit. This model was built with the program *O* (Jones *et al.*, 1991) and subjected to several rounds of crystallographic refinement with *CNS* (Brünger *et al.*, 1998) combined with model rebuilding. The two molecules in the asymmetric unit were refined separately, although NCS restraints were used during the early stages of refinement. $R_{\rm free}$ was calculated throughout the refinement process, using the same set of test reflections each time. The final model, refined to an R factor of 18.9% ($R_{\rm free}$ = 25.4%) at 2.7 Å resolution, showed good quality (Table 2) as judged with the program *PROCHECK* (Laskowski *et al.*, 1993) and had no residues in the disallowed regions of the Ramachandran plot. Fig. 1 provides an example of the quality of the final $2F_o - F_c$ electron-density map. Amino-acid sequences were obtained from the SWISS-PROT data bank (Bairoch & Apweiler, 2000).

Table 2
Refinement statistics.

Program	*CNS*
Resolution range (Å)	30–2.7
Data cutoff (σ)	2.0
No. of reflections	12624
Completeness (%)	88.4 (64.6)
No. of residues included†	426
Number of non-H atoms†	6672
Solvent (%)	53
R factor (%)	18.9 (32.1)
$R_{\rm free}$ (%)	25.4 (33.7)
Test-set size (%)	8.9 (7.3)
Mean B value (overall, Å^2)	53.0
Residues in allowed regions (%)	88.6
Residues in additionally allowed regions (%)	11.4
R.m.s. deviations from ideal values	
Bond lengths (Å)	0.014
Bond angles (°)	2.703

† Two crystallographically independent molecules in the asymmetric unit.

3. Results and discussion

3.1. Structure of L1 from *M. thermolithotrophicus*

The model of L1 from *M. thermolithotrophicus* contains two protein molecules, giving a total of 3336 non-H atoms. Each molecule contains 213 amino-acid residues and consists of two domains. The overall view of the MthL1 structure and the C$^\alpha$-atom trace are presented in Fig. 2. The N- and C-termini are close to each other in domain I. This domain spans residues 1–53 and 149–213, whereas domain II includes residues 54–148. The location of the secondary-structure elements within the sequence is shown in Fig. 3.

Domain I contains a four-stranded antiparallel β-sheet (β_1, β_8, β_9, β_{10}) flanked by two α-helices (α_1, α_8) on one side and exposed on the other. Strands β_2 and β_7 form a double-stranded antiparallel β-sheet, which is away from the main sheet of domain I and makes covalent connections to domain II. The connectivity scheme of domain I is $\alpha_1\beta_1\beta_2\beta_7\beta_8\alpha_8\beta_9\beta_{10}$ (Fig. 3). Loops β_1–β_2 and α_8–β_9 include residues in 3_{10}-helix conformation. The extended hydrophobic core of this domain contains 28 totally inaccessible residues, including five polar ones. The latter usually are involved in hydrogen bonds with the atoms of the main chain and stabilize the structure. Thus, Gln24 stabilizes the relative position of two loops α_1–β_1 and α_8–β_9 and Asn177 connects helix α_8 with loop β_2–β_3, whilst Thr201 links helix α_9 to helix α_1 and strand β_{10}. Residue Thr149 is hydrogen bonded to both the side and main chains of Arg145 and is involved in the net of hydrogen bonds connecting the two domains.

Domain II has an overall Rossmann fold topology with the connectivity scheme $\beta_3\alpha_2\beta_4\alpha_3\alpha_4\beta_5\alpha_5\alpha_6\beta_6\alpha_7$ (Fig. 3). It contains two α-helices (α_2, α_7) on one side of the four-stranded parallel β-sheet (β_3, β_4, β_5, β_6) and four α-helices (α_3, α_4, α_5, α_6) on the other. All these helices make a pseudo-cylinder, with the bases formed by helices α_2, α_3, α_4 and α_5, α_6, α_7. The β-sheet, which is inside the pseudo-cylinder, is approximately perpendicular to the bases. The hydrophobic core of domain II includes 25 totally inaccessible residues. The hydrophobic cores of both domains are connected with each other through residues Val49, Pro58, Phe104 and Leu151. The totally inaccessible polar residues of domain II form hydrogen bonds with both the main-chain and side-chain atoms and stabilize the structure. Thus, His102 links loop α_4–β_5 to helix α_4 and Gln108 connects the end of strand β_5 to the beginning of helix α_2, whereas Thr154 connects the end of strand β_7 to the beginning of strand β_2.

The surface of the MthL1 protein has several hydrophobic patches. The most extended (and rather flat) one includes residues Ala109, Met112, Pro113, Pro121, Pro125, Met129, Pro132 and Pro134. Three other patches are formed by Phe22, Met205, Met94, Ile98, Met1, Leu193 and the non-polar atoms of several nearby hydrophilic residues. The molecule contains 35 positively and 29 negatively charged residues. Four of them, located at helix α_1 and the C-terminus (Lys8, Glu12, Glu212 and Lys213), form a planar extended cluster (11 Å long) at the pole of the molecule.

The two molecules in the asymmetric unit have similar conformations, with an r.m.s. deviation between C$^\alpha$ atoms of 0.48 Å.

3.2. Comparison of MthL1, MjaL1 and TthL1 folds

The overall three-dimensional structure of MthL1 is closely related to that of MjaL1. Both structures were superimposed using the least-squares option of *O* with an r.m.s. deviation of 0.75 Å for all C$^\alpha$ atoms. Superposition of domains I yielded an r.m.s. deviation of 0.67 Å; that of domains II was 0.64 Å. Each domain of bacterial protein TthL1 is closely related topologically to the archaeal L1 proteins, although there are essential differences in the structures. Thus, TthL1 contains an additional 16 N-terminal residues which are partly folded into a 3_{10} helix, whereas the archaeal proteins possess seven extra residues in domain II, forming helix α_4 (Fig. 3). The bacterial and archaeal structures differ significantly in the relative arrangement of the α-helices and the β-sheets in domains I and II. As a result, C$^\alpha$ atoms of the MthL1 and TthL1 structures were superimposed with an r.m.s. deviation of about 3 Å for each of the domains. Sequence alignment based on

comparison of the bacterial and archaeal structures reveals two gaps in domain II between residues Pro130 and Asn138 (Fig. 3).

3.3. Two conformations of L1 proteins

In spite of the closely related topology of each domain in the three L1 structures, the overall shapes of archaeal and bacterial L1 proteins differ dramatically because of the different relative positions of domains I and II. In the MthL1 and MjaL1 structures, the relative orientation of the two domains is the same. It is stabilized by a net of hydrogen bonds and salt bridges as well as an extended hydrophobic core. Therefore, this conformation of the L1 proteins can be treated as a stable one.

In the TthL1 structure, the two domains form the interdomain cavity. This results in a closed conformation of TthL1 compared with the opened conformation of the archaeal proteins. The domains in TthL1 make only a few non-covalent interactions: this suggests flexibility of the structure (Nikonov *et al.*, 1996). The subsequent structure of the mutant S179C of the TthL1 protein clearly demonstrated the interdomain flexibility in TthL1 (Unge *et al.*, 1997). The mutant molecule displayed a small but significant opening of the cavity between the two domains, whereas the domain structures were essentially the same, with r.m.s. deviations of 0.77 and 0.31 Å for C^{α} atoms of domain I and domain II, respectively. Thus, the replacement of a single residue in the closed conformation of TthL1 changed the relative orientation of the domains, whereas the opened conformation was retained in MjaL1 and MthL1 even though about 29% of the residues in the corresponding sequences were different.

The two observed conformations of the L1 proteins could be caused by different crystal packing. However, crystals of MthL1 and MjaL1 belong to different space groups, with different numbers of molecules in the asymmetric unit. As a result, the crystal packing varies for these L1 proteins, but the opened conformation of both structures is highly conserved. At the same time, crystals of wild-type and mutant forms of TthL1 belong to the same space group and have closely related intermolecular interactions, but differ in the relative orientation of the domains. Thus, it is evident that the two different conformations are the inherent characteristic of the L1 proteins. Computer simulations show no evident restrictions that would prevent the closed conformation of TthL1 from adopting the same opened conformation as MthL1 and MjaL1 (Nevskaya *et al.*, 2000). This suggests that L1 proteins from different sources might adopt an opened conformation upon RNA binding.

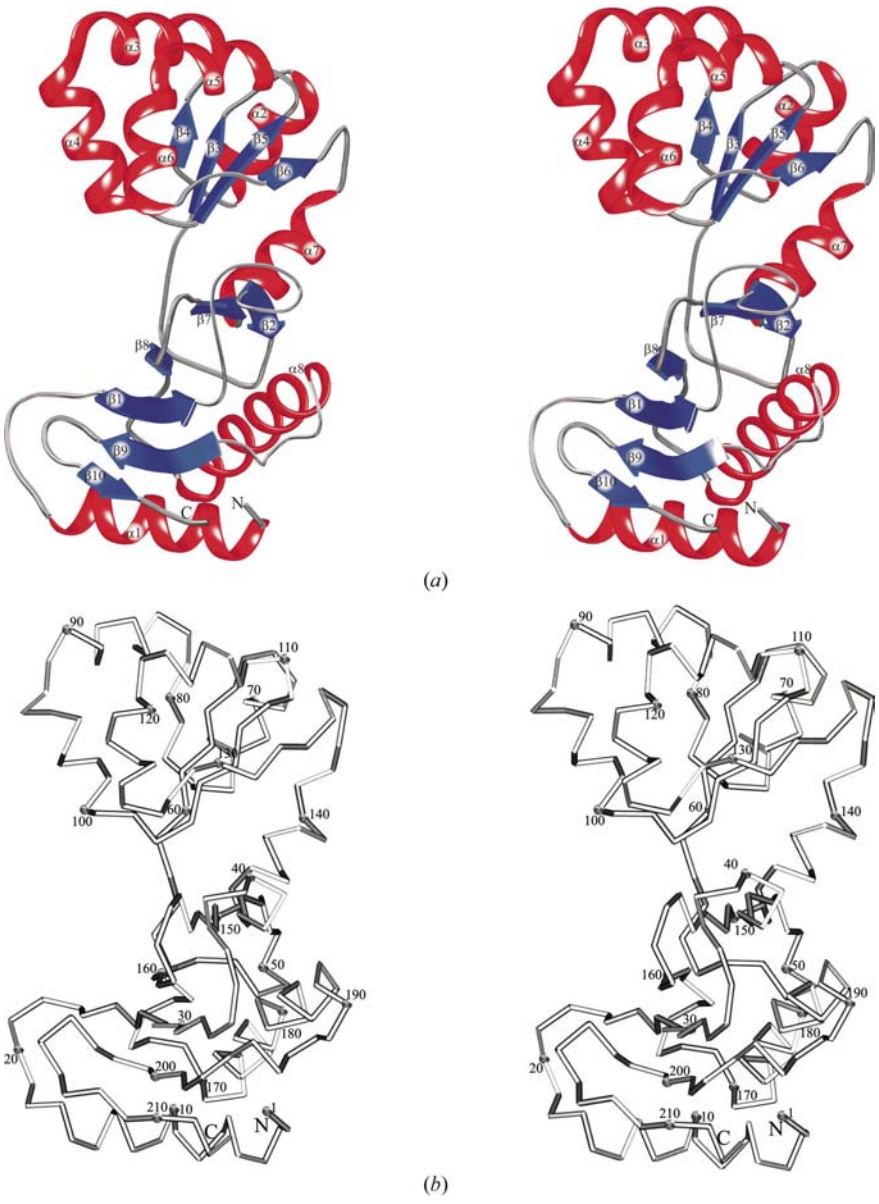

Figure 2
Overall structure of MthL1. (*a*) Stereo ribbon representation of the model. The β-strands are in blue and the α-helices are in red. (*b*) Stereo C^{α} trace of the MthL1 backbone with every tenth atom labelled and marked with a closed circle.

3.4. Comparison of intermolecular interactions in crystals of three L1 proteins

Each MthL1 molecule makes contacts with nine neighbouring molecules in the crystal (Table3). Both domains contribute to intermolecular interactions and the contact areas vary from 400 to 70 $Å^2$ per molecule. The molecules in the asymmetric unit interact with each other mainly through two large hydrophobic patches, formed both by hydrophobic residues and non-polar atoms of the nearest hydrophilic

Table 3
Intermolecular contacts in the MthL1 crystals.

No. of contact site	Contacting residues of original molecule	Assignment	Domain	Contact molecule	Contact area (Å^2)
1	Arg20, Asn21, Phe22, Thr204, Met205	Loop α_1–β_1, loop β_9–β_{10}	1	S1	280
2	Asn100, Glu101	Helix α_4	2	S1	100
3	Met112, Pro113, Gly116, Gly124, Met129, Pro132	Helix α_5, helix α_6, loop α_6–β_6	2	S2	280
4	Lys65, Gln82	Loop β_3–α_2, helix α_3	2	S2	100
5	Glu190, Lys191, Tyr194	Loop α_8–β_9	1	S3	310
6	Glu87, Lys90, Asn91, Lys93, Met94, Lys97	Helix α_3, helix α_4	2	S4	310
7	Arg39, Pro40, Glu41, Lys188, Gly190	Loop β_1–β_2, loop α_8–β_9	1	S5	250
8	Lys65, Gly66, Asp67, Ala70, Gln71, Glu73, Glu74, Arg81	Loop β_3–α_2, helix α_2, loop β_4–α_3	2	S6	250
9	Asn52, Lys168, Ser170, Glu172, Glu173	Loop β_2–β_3, loop β_8–α_8, helix α_8	1	S7	140
10	Glu4, Lys8	Helix α_1	1	S8	70
11	Asp156, Lys157	Loop β_7–β_8	1	S9	70

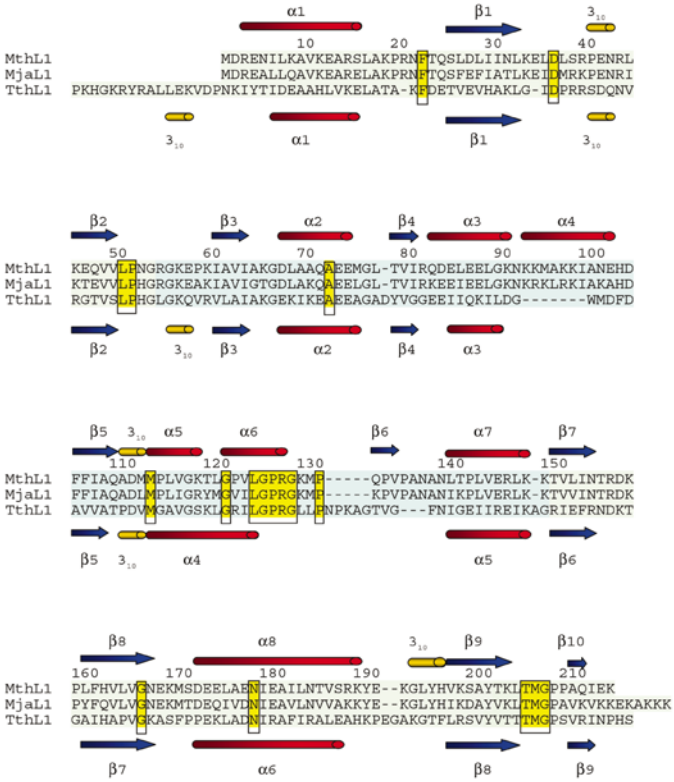

Figure 3
Sequence alignment of the three L1 proteins based on their structure comparison. The numbering corresponds to MthL1. Residues of domain I are shown with a light green background and residues of domain II with a light blue background. Residues identical in all known bacterial and archaeal sequences are boxed and shown with a yellow background. α-helices are shown as red cylinders, 3_{10}-helices as gold cylinders and β-sheets as blue arrows.

Table 4
Comparison of invariant regions in MthL1, MjaL1 and TthL1.

	R.m.s. deviation for C$^\alpha$ atoms	
Residues of MthL1	MjaL1/MthL1	TthL1/MthL1
Asn21, Phe22, Thr23, Gln24, Ser25, Leu203, Thr204, Met205	0.2	0.5
Met112, Pro113, Gly116, Leu123, Gly124, Pro125, Arg126, Gly127, Met129, Pro132	0.3	0.7
Arg39, Pro40, Glu41, Lys188, Gly190	0.4	2.3

residues of contact sites 1 and 3 (Table 3). The non-polar atoms also contribute to another large region of interaction of the two molecules (contact sites 5 and 6).

The contact sites on the surface of domain I can be integrated into two compact and one extended contact regions. Both compact regions are located at the domain poles and include the residues in loops α_1–β_1 and β_9–β_{10} (site 1) at one pole and loops β_1–β_2, α_8–β_9 (sites 5 and 7) on the other. The extended contact region is located on the α-helical side of domain I and includes contact sites 9, 10 and 11. All but one contact site on the surface of domain II (sites 2, 4, 6 and 8) could be integrated into the contacting region, located on one base of the pseudo-cylinder of the domain, whereas site 3 is located on its other base. Residues of the α-helices mainly contribute to the contact regions of domain II.

Detailed analysis of crystal packing in the crystals of L1 from *T. thermophilus* and *M. jannaschii* shows that the largest total contact area per molecule is in the MthL1 crystals (2200 Å^2) relative to that in TthL1 (1600 Å^2) and MjaL1 (990 Å^2). The lowest number of contacts is in the MjaL1 crystals belonging to space group *P*1 and almost all MjaL1 protein–protein binding regions are involved in the intermolecular interactions in the crystals of other two L1 proteins. That is the case for the two binding regions, located on both poles of domain I and on the base of domain II (helices α_5, α_6 and loop α_6–β_6).

Thus, analysis of the intermolecular contacts in the crystals of the L1 proteins from three sources reveals universal protein–protein contact regions in spite of different protein conformations and crystal packing. Such regions can be treated as universal binding sites for L1 proteins which could participate in protein–protein or RNA–protein interactions.

3.5. Structural invariants in L1 family proteins

The structures of each universal contact region in the MthL1, MjaL1 and TthL1 proteins were superimposed using the least-squares option of *O* (Jones *et al.*, 1991). The r.m.s. deviations for C$^\alpha$ atoms are represented in Table 4. The comparison revealed that all three structures coincide quite well in the regions located at one pole of domain I (loops α_1–β_1 and β_9–β_{10}) and at one base of domain II (helices α_5, α_6 and loop α_6–β_6). This is the case not only for the main-chain atoms but also for the side-chain atoms (Fig. 4). Thus, the surface of the L1 molecule contains two regions which are structurally very conserved. These structural invariants are involved in the intermolecular contacts in the crystals and

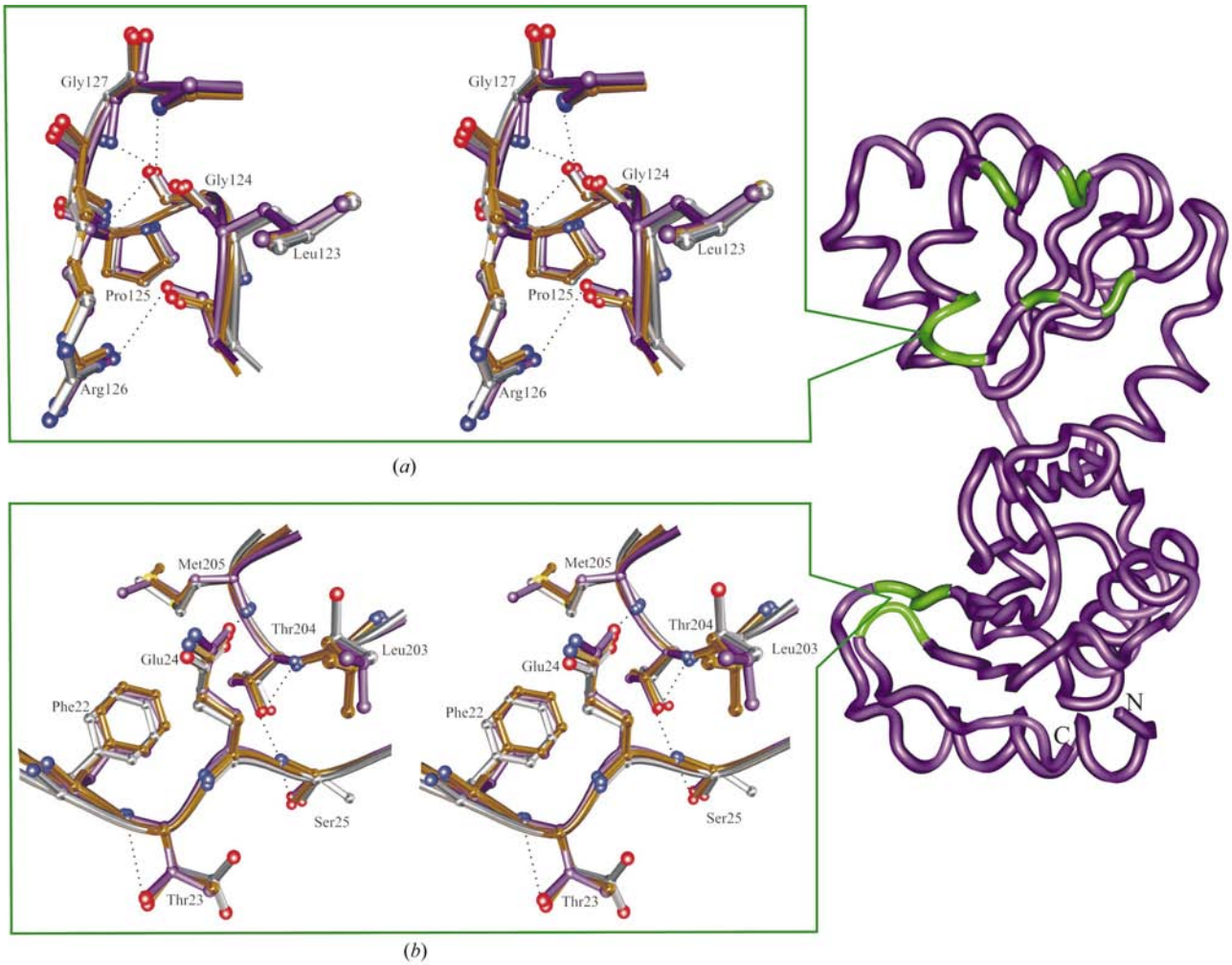

Figure 4
Two structural invariants on the surface of L1 proteins. The location of the invariants is shown in green on the MthL1 model (right). Superposition of the invariant regions in L1 proteins from three sources is shown at the left. MthL1 is in magenta, MjaL1 in brown and TthL1 in grey. Part of the invariant region, located on the base of domain II, is labelled (*a*). The invariant region on the pole of domain I, labelled (*b*), includes residues of two loops α_1–β_1 and β_9–β_{10}.

could be treated as biological contacts (Valdar & Thornton, 2001), which may be important for intermolecular interactions within the ribosome. Each structural invariant contains one cluster of conserved residues Phe22, Thr204, Met205 or Gly124, Pro125, Arg126, Gly127. The structures of the region located at the other pole of domain I (loops β_1–β_2 and α_8–β_9) coincide quite well for the archaeal proteins, but not for the bacterial protein, where loop α_8–β_9 is two residues longer.

It is known that L1 from *Escherichia coli* has the ability to bind specifically to a variety of bacterial and archaeal 23S rRNAs (Stanley *et al.*, 1978; Zimmermann, 1980; Baier *et al.*, 1989) as well as to eukaryal 26S/28S rRNAs (Gourse *et al.*, 1981). Moreover, it has been shown that for phylogenetically unrelated species such as *E. coli* and *M. vannielii* L1 proteins are functionally interchangeable within the ribosome as well as in repression of translation (Baier *et al.*, 1990; Hanner *et al.*, 1994). This suggests a structural similarity of both the RNA-binding site on L1 and the L1-binding site on the respective RNA molecules in various organisms (Sor & Nomura, 1987; Hanner *et al.*, 1994). The present comparative analysis of the three L1 structures (MthL1, MjaL1 and TthL1) and their crystal packing revealed two structural invariants on the L1 molecule surface which could be treated as the RNA-binding sites.

This work was supported by the Russian Academy of Sciences and the Russian Foundation for Basic Research. The research of MG was supported in part by a International Research Scholar's award from the Howard Hughes Medical Institute. The research of WP was supported by the Austrian Science Fund (FWF, P14550-GEN).

References

Baier, G., Hohenwarter, O., Hofbauer, C., Hummel, H., Stöffler-Meilicke, M. & Stöffler, G. (1989). *Syst. Appl. Microbiol.* **12**, 119–126.
Baier, G., Piendl, W., Redl, B. & Stöffler, G. (1990). *Nucleic Acids Res.* **18**, 719–724.
Bairoch, A. & Apweiler, R. (2000). *Nucleic Acids Res.* **28**, 45–48.

Ban, N., Nissen, P., Hansen, J., Capel, M., Moore, P. B. & Steitz, T. A. (1999). *Nature (London)*, **400**, 841–847.
Ban, N., Nissen, P., Hansen, J., Moore, P. B. & Steitz, T. A. (2000). *Science*, **289**, 905–920.
Branlant, C., Krol, A., Machatt, A. & Ebel, J.-P. (1981). *Nucleic Acids Res.* **9**, 293–307.
Brünger, A. T., Adams, P. D., Clore, G. M., DeLano, W. L., Gros, P., Grosse-Kunstleve, R. W., Jiang, J.-S., Kuszewski, J., Nilges, M., Pannu, N. S., Read, R. J., Rice, L. M., Simonson, T. & Warren, G. L. (1998). *Acta Cryst.* D**54**, 905–921.
Esnouf, R. M. (1999). *Acta Cryst.* D**55**, 938–940.
Gourse, R. L., Sharrock, R. A. & Nomura, M. (1986). *Structure, Function and Genetics of Ribosomes*, edited by B. Hardesty & G. Kramer, pp. 766–788. New York: Springer–Verlag.
Gourse, R. L., Thurlow, D. L., Gerbi, S. A. & Zimmermann, R. A. (1981). *Proc. Natl Acad. Sci. USA*, **78**, 2722–2726.
Hanner, M., Mayer, C., Köhrer, C., Golderer, G., Gröbner, P. & Piendl, W. (1994). *J. Bacteriol.* **176**, 409–418.
Jones, T. A., Zou, J.-Y., Cowan, S. W. & Kjeldgaard, M. (1991). *Acta Cryst.* A**47**, 110–119.
Köhrer, C., Mayer, K., Neumair, O., Gröbner, P. & Piendl, W. (1998). *Eur. J. Biochem.* **256**, 97–105.
Kraft, A., Lutz, C., Lingenhel, A., Gröbner, P. & Piendl, W. (1999). *Genetics*, **152**, 1363–1372.
Kraulis, P. J. (1991). *J. Appl. Cryst.* **24**, 946–950.
Laskowski, R. A., MacArthur, M. W., Moss, D. S. & Thornton, J. M. (1993). *J. Appl. Cryst.* **26**, 283–291.
Matthews, B. W. (1968). *J. Mol. Biol.* **33**, 491–497.
Navaza, J. (1994). *Acta Cryst.* A**50**, 157–163.
Nevskaya, N., Tishchenko, S., Fedorov, R., Al-Karadaghi, S., Liljas, A., Kraft, A., Piendl, W., Garber, M. & Nikonov, S. (2000). *Structure*, **8**, 363–371.
Nikonov, S., Nevskaya, N., Eliseikina, I., Fomenkova, N., Nikulin, A., Ossina, N., Garber, M., Jonsson, B.-H., Briand, C., Al-Karadaghi, S., Svensson, A., Aevarsson, A. & Liljas, A. (1996). *EMBO J.* **15**, 1350–1359.
Otwinowski, Z. & Minor, W. (1997). *Methods Enzymol.* **276**, 307–326.
Sor, F. & Nomura, M. (1987). *Mol. Gen. Genet.* **210**, 52–59.
Stanley, J., Sloof, P. & Ebel, J.-P. (1978). *Eur. J. Biochem.* **85**, 309–316.
Tishchenko, S., Nikonov, S., Garber, M., Kraft, A., Köhrer, C. & Piendl, W. (1998). *Biochem. Mol. Biol. Int.* **45**, 349–354.
Unge, J., Al-Karadaghi, S., Liljas, A., Jonsson, B.-H., Eliseikina, I., Ossina, N., Nevskaya, N., Fomenkova, N., Garber, M. & Nikonov, S. (1997). *FEBS Lett.* **411**, 53–59.
Valdar, W. S. J. & Thornton, J. M. (2001). *J. Mol. Biol.* **313**, 399–416.
Yusupov, M. M., Yusupova, G. Zh., Baucom, A., Lieberman, K., Earnest, T. N., Cate, J. H. D. & Noller, H. F. (2001). *Science*, **292**, 883–896.
Zimmermann, R. A. (1980). *Ribosomes. Structure, Function and Genetics*, edited by G. Chambliss, G. R. Craven, J. Davies, K. Davies, L. Kahan & M. Nomura, pp. 135–169. Baltimore: University Park Press.
Zimmermann, R. A., Thurlow, D. L., Finn, R. S., Marsh, T. L. & Ferrett, L. K. (1980). *Genetics and Evolution of RNA Polymerase, tRNA and Ribosomes*, edited by S. Osava, H. Ozeki, H. Uchida & T. Yura, pp. 569–584. Tokyo: University of Tokyo Press.